Research Article

MOLECULAR PAIN

Molecular Pain
Volume 13: 1–18

DOI: 10.1177/1744806917717040
journals.sagepub.com/home/mpx
SAGE

Primary sensory neuron-specific interference of TRPV1 signaling by adeno-associated virus-encoded TRPV1 peptide aptamer attenuates neuropathic pain

Hongfei Xiang[1,2], Zhen Liu[1], Fei Wang[1,3], Hao Xu[1,2], Christopher Roberts[1], Gregory Fischer[1], Cheryl L Stucky[4], Caron Dean[1,5], Bin Pan[1], Quinn H Hogan[1,5] and Hongwei Yu[1,5]

Abstract

Background: TRPV1 (transient receptor potential vanilloid subfamily member 1) is a pain signaling channel highly expressed in primary sensory neurons. Attempts for analgesia by systemic TRPV1 blockade produce undesirable side effects, such as hyperthermia and impaired heat pain sensation. One approach for TRPV1 analgesia is to target TRPV1 along the peripheral sensory pathway.

Results: For functional blockade of TRPV1 signaling, we constructed an adeno-associated virus (AAV) vector expressing a recombinant TRPV1 interfering peptide aptamer, derived from a 38mer tetrameric assembly domain (TAD), encompassing residues 735 to 772 of rat TRPV1, fused to the C-terminus of enhanced green fluorescent protein (EGFP). AAV-targeted sensory neurons expressing EGFP-TAD after vector injection into the dorsal root ganglia (DRG) revealed decreased inward calcium current and diminished intracellular calcium accumulation in response to capsaicin, compared to neurons of naïve or expressing EGFP alone. To examine the potential for treating neuropathic pain, AAV-EGFP-TAD was injected into fourth and fifth lumbar (L) DRGs of rats subjected to neuropathic pain by tibial nerve injury (TNI). Results showed that AAV-directed selective expression of EGFP-TAD in L4/L5 DRG neuron somata, and their peripheral and central axonal projections can limit TNI-induced neuropathic pain behavior, including hypersensitivity to heat and, to a less extent, mechanical stimulation.

Conclusion: Selective inhibition of TRPV1 activity in primary sensory neurons by DRG delivery of AAV-encoded analgesic interfering peptide aptamers is efficacious in attenuation of neuropathic pain. With further improvements of vector constructs and *in vivo* application, this approach might have the potential to develop as an alternative gene therapy strategy to treat chronic pain, especially heat hypersensitivity, without complications due to systemic TRPV1 blockade.

Keywords

Transient receptor potential vanilloid 1, neuropathic pain, dorsal root ganglion, primary sensory neurons, adeno-associated virus, gene therapy

Date received: 29 January 2017; revised: 11 April 2017; accepted: 24 April 2017

[1]Department of Anesthesiology, Medical College of Wisconsin, Milwaukee, WI, USA
[2]Department of Orthopedic Surgery, Affiliated Hospital of Qingdao University, Qingdao, China
[3]Medical Experiment Center, Shaanxi University of Chinese Medicine, Xianyang, China
[4]Department of Cell Biology, Neurobiology and Anatomy, Medical College of Wisconsin, Milwaukee, WI, USA
[5]Zablocki Veterans Affairs Medical Center, Milwaukee, WI, USA

Corresponding authors:
Hongwei Yu and Quinn H Hogan, Department of Anesthesiology, Medical College of Wisconsin, 8701 Watertown Plank Road, Milwaukee, WI 53226, USA.
Emails: hyu@mcw.edu; qhogan@mcw.edu

Introduction

Chronic pain represents a major health challenge.[1] Large strides have been made in understanding mechanisms underlying neuropathic pain.[2] This includes the identification of the TRPV1 (transient receptor potential vanilloid 1), a member of the vanilloid receptors that are highly expressed in primary sensory neuron somata and their fibers, as an important cellular integrative sensor for detecting noxious stimuli and transducing pain signals in the settings of various types of chronic pain.[3–7] However, therapy by systemic TRPV1 blockade is accompanied by hyperthermia and impaired heat pain sensation,[8,9] so an approach that can selectively block affected pain pathways is needed. Growing evidence shows that TRPV1 nociception in primary sensory neurons depends on its interaction with many other molecules, which together comprise the TRPV1 interactome.[10–13] Genetically disrupting these interactions is an innovative strategy for the treatment of chronic pain,[14–17] which combined with anatomically selective delivery may offer a primary sensory neuron-specific approach.

Interfering peptide aptamers (iPAs) are designed as a short fragment of endogenous protein, encompassing a domain with high affinity and specificity for binding to cognate sites of target proteins, thereby functioning as a decoy molecule that blocks protein–protein interaction and induces selective interference of the target protein function.[18] Several studies have described a number of TRPV1-derived iPAs that are mapped to the transient receptor potential box of cytosolic proximal part of TRPV1 C-terminus. These iPAs exert dominant-negative effects on TRPV1 functions by interfering with protein folding, trafficking, subunit assembly, and/or desensitizing TRPV1 binding to interaction molecules.[14–17,19–21]

To form functional cation-permeable pores, TRPV1 subunits need to tetramerize in cell membrane via specialized peptide motifs functioning as the tetrameric assembly domains (TAD) mainly located at the TRPV1 cytosolic C terminus.[20,22–25] Although iPAs derived from TAD can selectively inhibit TRPV1 function and transiently reduce hypersensitive behavior in pain animal models,[15,16] pharmacological application of membrane-permeable iPAs (i.e., iPAs fused to cell-penetrating peptide) is hampered by their low stability and proteolytic lability in cells, and systemic peptide therapy cannot restrict the iPAs to the neural pathways responsible for transduction and transmission of nociceptive signals. As a result, potential off-target effects unrelated to pain can prevent sufficient dosing for effective antinociception, as in the case of hyperthermia from systemic TRPV1 blockade. Ideally, the therapeutic iPAs should be restricted *in situ* to the pathological sites, should be produced at stable concentrations that are sufficient to desensitize hyperactive pain signaling, and should have effects that are adequately sustained to avoid the need for frequently repeated injections. Gene therapy is a suitable strategy to achieve these outcomes, with recombinant adeno-associated virus (AAV) demonstrating promise as one of the gene delivery tools for targeted applications.[18,26]

Here, we combine a genetic strategy using AAV to transfer and persistently express a fluorescent TAD chimera (enhanced green fluorescent protein (EGFP)-TAD) selectively in primary sensory neurons, with an anatomic strategy for segmentally targeting neurons at the level of the painful condition via injection into the dorsal root ganglia (DRG), which has been shown to be a safe procedure in both rats and humans.[27,28] We show that selective expression of TRPV1 TAD in lumbar (L) L4/L5 DRG neurons and their axonal projections provides effective and sustained attenuation of neuropathic pain induced by tibial nerve injury (TNI).

Materials and methods

Animals

Experiments were performed in adult male Sprague-Dawley rats (five–six weeks old; 125–150 g body weight) purchased from Charles River Laboratories (Wilmington, MA). All animal procedures were reviewed and approved by the Animal Care Committee of the Zablocki VA Medical Center Animal Studies Subcommittee and the Medical College of Wisconsin IACUC (Permission number: 3690-03). Rats were housed in standard 12-h cycle lighting and were allowed ad libitum access to food and water prior to and throughout the experimental protocol.

Construct and AAV production

To construct the AAV vector coding a chimeric EGFP-TAD expression cassette, we subcloned a DNA fragment encoding a 38mer peptide ranging the residues 735 to 772 of rat TRPV1 into *BsrG*I/*Sal*I sites of a single-strand AAV expressing plasmid pAAV-CMV-EGFP (Cell Biolabs, San Diego, CA). This generated pAAV-CMV-EGFP-TAD that codes the EGFP-TAD fusion protein under the transcriptional control of the CMV promoter (Supplementary Figure S1(a)). The construct was sequenced to confirm the desired sequence and the correct reading frame. Plasmids pAAV-CMV-EGFP-TAD and pAAV-CMV-EGFP were used to package AAV2/6-EGFP-TAD and AAV2/6-EGFP as a control (subsequently referred to as AAV6-TAD and AAV6-EGFP, respectively) for *in vivo* injection. AAV vectors were produced and purified in our laboratory by previously described methods.[26] This included AAV particle purification by optiprep ultracentrifugation and concentration by use of Centricon Plus-20 (Regenerated Cellulose 100,000 MWCO, Millipore, Billerica, MA).

AAV titer was determined by PicoGreen (life technologies, Carlsbad, CA) assay, and final aliquots were kept in $1\times$ phosphate buffered saline containing 5% sorbitol (Sigma-Aldrich, St. Louis, MO) and stored at -80°C. The titers of AAV6-TAD and AAV6-EGFP vectors were 1.04×10^{13} GC/ml and 1.0×10^{13} GC/ml, respectively. The same lot of viral preparation was used for all *in vivo* experiments. Vectors were evaluated for purity by sodium dodecyl sulfate polyacrylamide gel (SDS-PAGE) electrophoresis followed by silver stain using a Pierce silver stain kit (Fisher Scientific, Rockford, IL) according to manufacturer's protocol. Comparable purity of AAV6-TAD and control AAV6-EGFP was confirmed by silver staining showing dominant viral Vp1, Vp2, and Vp3 proteins (95% for AAV6-TAD and 88% for AAV6-EGFP) (Supplementary Figure S1(b)). Infectivity was estimated by evaluating the percentage of EGFP-positive HEK293T cells 48 h after transduction of either AAV6-EGFP-TAD or AAV6-EGFP at a multiplicity of infection of 10,000 (Supplementary Figure S1(c)). By immunoblotting, the EGFP-TAD chimeric protein stable expression was confirmed in the lysates of HEK293T cells transduced with AAV6-EGFP-TAD with a mass that is ~10 kDa larger than EGFP (Supplementary Figure S1(d)).

Microinjection of AAV vectors into DRGs

Nearly all of the sciatic DRG perikarya resided in the L4 and L5 DRGs.[29] AAV vector was microinjected into right L4 and L5 DRGs using previously described techniques.[27] In brief, the surgically exposed intervertebral foramen was minimally enlarged by removal of laminar bone. The injection was performed through a micropipette that was advanced approximately 100 μm into the ganglion. Rats received L4 and L5 DRG injections of either AAV6-TAD or AAV6-EGFP (one vector per rat), consisting of 2 μl with adjusted titers containing a total of 2.0×10^{10} GC particles. The injection was performed over a 5 min period using a Nanoliter 2000 microprocessor-controlled injector (World Precision Instruments, Sarasota, FL). Removal of the pipette was delayed for an additional 5 min to minimize extrusion of the injectate. Following the injection and closure of overlying muscle and skin, the animals were returned to the animal house where they remained for the experimental times. We have previously shown that AAV6 administered in this fashion produce transduction limited to the neurons of the injected DRGs, without significant glial transduction, likely due to high purity of vectors.[18,26]

Tibial nerve injury

To model clinical traumatic painful peripheral neuropathy, we performed a TNI, an established model of peripheral nerve injury that is less severe than spared nerve injury.[30,31] Animals were anesthetized using isoflurane at 4% induction and 2% maintenance. Under anesthesia, the right sciatic nerve was isolated under aseptic surgical conditions by blunt dissection of the femoral biceps muscle. The sciatic nerve and its three branches were isolated (sural, common peroneal, and tibial nerves), and only the tibial nerve was tightly ligated and transected distal to the ligation. The overlying muscle and skin were then sutured following surgery. Sham-operated rats were subjected to all preceding procedures without nerve ligation and transection.

Pain behavioral evaluation

Behavioral tests were performed in a blinded fashion. Animals were habituated in individual test compartments for at least 1 h before each testing. Stimuli were applied to the lateral margin of the plantar aspect of the foot in the sural area of innervation.

1. Mechanical allodynia: Mechanical withdrawal threshold testing (von Frey test) was performed using calibrated monofilaments (0.3, 0.5, 0.8, 1.0, 2.8, 5, 9, 14, and 24 g, Patterson Medical, Bolingbrook, Illinois). Animals were habituated in individual test compartments in an elevated mesh-bottomed platform with a grid for at least 1 h before testing. Beginning with the 2.8 g filament, filaments were applied to the plantar skin with just enough force to bend the fiber and held for 1 s. If a response was observed, the next smaller filament was applied, and if no response was observed, the next larger was applied, until a reversal occurred, defined as a withdrawal after a previous lack of withdrawal, or vice versa. Following a reversal event, four more stimulations were performed following the same pattern. The forces of the filaments before and after the reversal, and the four filaments applied following the reversal, were used to calculate the von Frey threshold. Rats not responding to any filament were assigned a score of 25 g.
2. Mechanical hyperalgesia (Pin test): Noxious punctate mechanical stimulation was performed using the point of a 22 g spinal anesthesia needle that was gently applied to the center of plantar surface of the hindpaw without penetrating the skin. Five applications were separated by at least 10 s, which was repeated after 2 min, making a total of 10 touches. For each application, the induced behavior was a very brisk, simple withdrawal with immediate return of the foot to the cage floor, or a sustained elevation with grooming that included licking and chewing, and possibly shaking, which lasted at least 1 s. This hyperalgesic behavior is specifically associated with place avoidance.[32]

Hyperalgesia was quantified by tabulating hyperalgesia responses as a percentage of total touches.

3. Heat nociception (Hargreaves test): This was performed using a device designed for the purpose of identifying heat sensitivity (Paw Thermal Stimulator System, University Anesthesia Research & Development Group, San Diego, CA). Rats were placed on a temperature-regulated glass platform heated to 30°C, and the lateral plantar surface of hind paws stimulated with a radiant heat source (50 W halogen bulb) directed through an aperture. The time elapsed from initiation of the stimulus until withdrawal (withdrawal latency) as detected by a series of photocells was measured. Each hind paw was tested four times, and the withdrawal latency values averaged.

Cutaneous capsaicin-induced behaviors

An acute cutaneous inflammation was induced by hindpaw intradermal injection of 10 µg capsaicin (8-methyl-N-vanillyl-6-nonamide, Sigma-Aldrich), prepared in a solution of 7% Tween 80 and 93% saline as previously described.[33] Animals were briefly anesthetized with isoflurane before injection to minimize their suffering. Capsaicin was injected into the plantar surface of the hindpaw in a volume of 10 µl. Immediately after injection, paw withdrawal responses to the 9 g von Frey monofilament in 10 times for a duration of 1 s with an inter-stimulus interval of approximately 1 s and to radiant heat applied on plantar skin were tested at 15, 30, 45, and 60 min. Paw withdrawal frequency (%) to von Frey stimulation was calculated as the numbers of paw withdrawals in 10 tests × 100. Only immediate, robust withdrawal responses from the von Frey stimulation were recorded as positive responses. Control experiments were done by vehicle injections using Tween 80 saline vehicle at the same volume as the capsaicin solution.

Immunohistochemistry

Immunohistochemistry staining was performed by a standard immunofluorescent labeling protocol, as previously described.[34] Briefly, the ipsilateral and contralateral DRGs, the corresponding levels of the spinal cord, the sciatic nerve at middle thigh level, and hindpaw glabrous skin were removed and fixed in 10% neutral buffered formalin, embedded with paraffin, and processed into a series of 5 µm sections. Sections were deparaffinized and rehydrated, and antigen retrieval was achieved by microwave heating in 10 mM citrate buffer (pH 6.0). Following primary antibodies or IB4 were used for colocalization immunostaining: monoclonal GFP (1:400, Santa Cruz Biotechnology, SCB, Santa Cruz, CA), mouse monoclonal β3-tubulin (1:500, SCB), mouse monoclonal calcitonin gene-related peptide (1:600, SCB), rabbit polyclonal TRPV1 (1:500, ThermoFisher, Waltham, MA), or Alexa 594 conjugated isolectin GS-IB4 (IB4, 1 µg/ml, Life Technologies), with normal immunoglobulin G (IgG from same species as the first antibody) replacement of first antibody as the negative control. The appropriate fluorophore-conjugated (Alexa 488 or Alexa 594) secondary antibodies (Jackson Immunoresearch, West Grove, PA) were used to reveal the immune complex. The sections were examined, and images captured using a Nikon TE2000-S fluorescence microscope equipped with an Optronics QuantiFire digital camera with filters suitable for selectively detecting the green, red, and blue fluorescence. For double-label colocalization, images from the same section but showing different antigen signals (different colors) were captured separately and overlaid. Colocalization was deemed for two proteins in areas stained with the combined color when the two images were overlaid.

Western blotting

Lysates of HEK293T cells and DRGs were extracted using 1 × radioimmunoprecipitation assay (RIPA) buffer (20 mm Tris-HCl pH 7.4, 150 mm NaCl, 1% Nonidet P-40, 1% sodium deoxycholate, 0.1% SDS, with 0.1% Triton X100 and protease inhibitor cocktail). Protein concentration determined by using the BCA kit (Pierce, Rockford, IL). Western blotting of cell and DRG lysates (20 µg protein) was preceded by SDS-PAGE gel electrophoresis, transferred onto nitrocellulose, and probed with a polyclonal rabbit anti-GFP antibody (1:1,000; Cell Signaling, Danvers, MA) or rabbit polyclonal TRPV1 (1:500, ThermoFisher). Immunoreactive proteins were detected by enhanced chemiluminescence (Pierce, Rockford, IL) after incubation with horseradish peroxidase-conjugated secondary antibodies (1:2000, SCB) and exposed to photographic film. Glyceraldehyde 3-phosphate dehydrogenase was used as a loading control. Densitometric analysis of TRPV1 protein levels in DRG homogenates was performed using ImageJ v.1.46. All samples were normalized to glyceraldehyde 3-phosphate dehydrogenase (GAPDH) as control.

Calcium imaging

Capsaicin-evoked increases of intracellular calcium levels ($[Ca^{2+}]_c$) were compared in small to medium (25–40 µm in diameter) L4 and L5 DRG neurons dissociated from naïve rats and animals injected with AAV6-TAD or AAV6-EGFP. Dissociated neurons cultured in coverslips were loaded with Fura-2-AM (5 µM) and maintained in

Tyrode's solution containing (in mM): NaCl 140, KCl 4, $CaCl_2$ 2, glucose 10, $MgCl_2$ 2, and 4-(2-hydroxyethyl)-1-piperazineethanesulfonic acid (HEPES) 10, with an osmolarity of 297 to 300 mOsm and pH 7.4. Recording was performed within 6 h of dissociation. Transduced neurons were identified by EGFP fluorescence. Capsaicin (50 nM and 100 nM) was applied locally (flow rate approximately 3/min) via a fine pipette positioned close to the cell being studied. The fluorophore was excited alternately with 340 nm and 380 nm wavelength illumination, and images were acquired at 510 nm using a cooled 12-bit digital at a rate of 3 Hz. The fluorescence ratio R for individual neurons was determined as the intensity of emission during 340 nm excitation (I_{340}) divided by I_{380}, and the Ca^{2+} concentration was estimated by as $(K_d)(\beta)(R–R_{min})/(R_{max}–R)$, where β is the ratio of I_{380} at zero and saturating Ca^{2+} concentrations. Values of R_{min}, R_{max}, and β were determined by in-situ calibration and were 0.38, 8.49 and 9.54, and Kd was 224 nm.[35] Plasma membrane Ca^{2+}-ATPase influence was eliminated by applying Tyrode's with pH 8.8 during depolarization, while stable intracellular $[Ca^{2+}]_c$ was maintained by simultaneously reducing bath Ca^{2+} concentration to 0.25 mM.

Voltage clamp of dissociated DRG neurons

After dissection in cold Ca^{2+}/Mg^{2+}-free HBBS (Life Technologies), ganglia were chopped, followed by incubating in 0.5 mg/ml liberase TM (Roche, Indianapolis, IN) in DMEM/F12 with glutaMAX (Life Technologies) for 30 min at 37°C, then with 1 mg/ml trypsin (Sigma-Aldrich) and 150 Kunitz units/ml DNase (Sigma-Aldrich) for another 10 min. After addition of trypsin inhibitor (Type II, Sigma-Aldrich), tissues were centrifuged, lightly triturated in neural basal media (1X) (Life Technologies) containing 2% (v:v) B27 supplement (50X) (Life Technologies), 0.5 mM glutamine (Sigma-Aldrich), 0.05 mg/ml gentamicin (Life technologies), and 10 ng/ml nerve growth factor 7S (Alomone Labs Ltd., Jerusalem, Israel). Cells were then plated onto poly-L-lysine (70–150 kDa, Sigma-Aldrich) coated coverslips and cultured at 37°C in 5% CO_2. All neurons were studied 3 to 8 h after dissociation. Small to medium sensory neurons (25–40 μm in diameter) were used for this study. Electrodes with a resistance of 2 to 4 MΩ were pulled from borosilicate glass (Garner Glass Co., Claremont, CA) using a micropipette puller (P-97 Sutter Instrument Co; Novato, CA, USA) and fire polished. Recording was performed in the whole-cell configuration with an Axopatch 700B amplifier (Molecular Devices, Sunnyvale, CA). After whole-cell configuration was established, electrical compensation for the cell membrane capacitance and series resistance were initiated. Access resistance was typically between 5 and 7 MΩ and was 80% to 90% compensated. Since peak currents measured in our experiment were around 3 nA, voltage errors introduced by the residual uncompensated access resistance (<1.0 MΩ) were <3 mV and could not introduce major errors. Neurons with >10 MΩ access resistance after breakthrough were discarded. Experiments were performed 5 min after breakthrough, and at room temperature (~25°C). Signals were filtered at 2 kHz through a four-pole Bessel filter and digitized at 10 kHz with a Digidata 1440A A/D interface (Molecular Devices). Seals were achieved in modified Tyrode's consisting of (in mM) NaCl 140, KCl 4, $CaCl_2$ 2, $MgCl_2$ 2, D-glucose 10, HEPES 10 at pH of 7.4, and with an osmolarity of 300 mOsm. Capsaicin (100 nM)-induced currents flowing through Ca^{2+} channels (I_{Ca}) were recorded using an extracellular solution consisting of (in mM) $BaCl_2$ 2, 4-aminophyridine 1, HEPES 10, tetraethylammonium chloride 140, HEPES 10 at pH of 7.4, and with an osmolarity of 300 mOsm. The internal pipette solution contained (in mM) CsCl 110, tetraethylammonium chloride 20, Mg-ATP 4, Na-GTP 0.3, ethylene glycol-bis(2-amino-ethylether)-N,N, N′, N′-tetra-acetic acid 11, $CaCl_2$ 1, $MgCl_2$ 1, 4 Mg-ATP, 0.4 Li_4-GTP, HEPES 10 at pH of 7.2, and with an osmolarity of 300 mOsm. Data from whole-cell I_{Ca} recordings were evaluated with Axograph X 1.3.5 (AxoGraph Scientific, Sydney, Australia), with which peak inward currents and charge transfer were measured. To correct for cell size, inward currents are expressed as a function of cell capacitance (pA/pF).

In vivo *electrophysiological recordings of DH neurons*

Rats were anesthetized with sodium pentobarbital (50 mg/kg, i.p.) with a catheter inserted into a femoral vein for supplemental administration of anesthetic doses (2 mg/kg, i.v.). Arterial blood pressure was monitored continuously using a PA-C10 transmitter (Data Sciences International (DSI), St. Paul, MN) inserted into a femoral artery. The trachea was cannulated through a midline cervical incision for ventilation with room air (Harvard 683 respirator), pneumothoraxes performed, and the rat was paralyzed with pancuronium bromide (0.1 mg/kg i.v, with supplemental doses of 0.01 mg/kg administered when spontaneous breathing was observed) prior to laminectomy. A surgical plane of anesthesia was reached prior to administration of pancuronium, as indicated by stability of blood pressure during stimulation. Supplemental doses of anesthetic were administered as indicate according to blood pressure changes. A heating pad was used to maintain body temperature at 37°C. For extracellular DH neuronal recordings, a laminectomy was performed from the T13 to the L3 vertebrae to expose the mid-lumbar

spinal cord, and a stabilizing stereotaxic clamp was applied to the spinal process rostral to the exposure. The dura was opened, and the cord was covered in warm mineral oil. First, activity evoked by mechanical stimulation of the receptive field was recorded. A single-barreled glass micropipette containing a carbon filament (7 μm diameter) for recording was advanced into the spinal cord using a microdrive, targeting lamina IV to VI of the L4 to L5 level at depths of 300 to 600 μm from the cord surface. Wide dynamic range neurons that responded to non-noxious and noxious stimulation in a graded manner were selected for study. Sequentially, the ipsilateral hindpaw was stimulated using cotton tip (stroking for 1 s at 0.5 Hz for 20 s), graded von Frey fibers (forces 0.07 g, 1.14 g, 8.0 g, and 60 g, each applied for 1 s at 0.5 Hz for 20 s), and venous clamp and arterial clamps that apply mild and moderate pinching force (each applied for 10 s one time). The various stimuli were applied following a 3 min rest interval. After recording evoked activity, spontaneous neuronal activity was recorded at two different longitudinal sites within the L4/5 recording area, and at four specified depths (300, 400, 500, and 600 μm from the cord surface) at each location, for 1 min at each location. This design was chosen to avoid sampling bias by going to these prespecified recording locations without reference to evocable activity.

Electrophysiological signals were directed to high impedance differential amplifiers (gain = 1000; 0.1–10 kHz passband), followed by filter/amplifiers (gain up to 400; high and low pass filtering 10 Hz–3 kHz). The amplifier output was displayed online and also directed to precision full-wave rectifiers and averaged using Bessel linear averaging filters (averaging interval = 100 mS) to obtain an online moving time average. Neuronal activity and the moving time average were continuously displayed/recorded along with arterial blood pressure with the CED Power 1401 mk II and Spike2 data acquisition system (Cambridge Electronic Design Limited, Cambridge, UK). Action potentials were isolated by setting the threshold above background noise, and individual units were identified by template matching using Spike2.

Statistical analysis

All statistical analysis was performed using Prism program (GraphPad Software, La Jolla, CA). Behavioral changes over time were analyzed by repeated measures parametric two-way analysis of variance (ANOVA) for von Frey and heat tests followed by Tukey's *post hoc* test for multiple comparisons, and non-parametric Friedman's ANOVA for pin test followed by Dunn's *post hoc* test. For comparisons between groups, the effects of vector injection were characterized by area under the curve analysis. Specifically, for Early Treatment, measured behavioral values after the combined injury and vector injection were normalized to the values immediately preceding injury and injection. For Late Treatment (in which vector injection was performed 14 days after nerve injury), measured values after the vector injection were normalized to the values immediately before the injection. Calculated area under the curves were compared between vectors by Student's *t* test for von Frey and heat and by Mann–Whitney U test for Pin. In electrophysiology experiments of DH neurons, baseline levels of neuronal spontaneous and evoked firing in rats were compared using Student's *t* test. Statistical differences in the experiments of measurement of cytoplasmic Ca^{2+} concentration, whole-cell patch-clamp recording, and TRPV1 expression by immunoblots were analyzed by one-way ANOVA followed by Tukey's *post hoc* test. Data were expressed as means ± SEM. A probability of $p < 0.05$ was considered as statistically significant.

Results

Construct design of AAV encoding TAD

TRPV1 is a tetrameric integral membrane protein, and its subunit organization and function are facilitated by interactions among C-terminal cytoplasmic domains,[19,20,36–38] which contain the essential tetramerization sequence of TRPV1. Therefore, we aimed to block TRPV1 assembly by expressing TAD in the cytoplasm of DRG neurons. Two adjacent small peptide motifs mapped to TRPV1 cytosolic C-terminus (amino acids ranging 735–752 and 752–772, respectively), which are overlapped from each other by one amino acid, have been independently defined in prior reports as the critical TRPV1 TAD.[16,19] Hence, we constructed an AAV encoding a 38mer TAD peptide (TRPV1 aa735–772), which was fused to EGFP in order to provide both a stable scaffold and a fluorescent tag for identifying neurons expressing EGFP-TAD driven under the cytomegalovirus (CMV) promoter. It is known that TRPV1 is highly expressed in various subtypes of primary sensory neurons, including C, Aδ, and some Aβ, and is distributed by axonal transport to both central presynaptic and peripheral terminals, although relatively limited TRPV1 expression in spinal cord interneurons and descending supraspinal fibers has recently been reported.[39–41] AAV was packaged as serotype 6, because we have previously shown that after intraganglionic delivery, the AAV6 serotype provides efficient gene transfer to the full range of DRG neurons, including the nociceptive sub-populations and their axonal terminals, and highly purified AAV6 with ubiquitous cell-potent CMV promoter leads to gene transfer predominantly to neurons without significant glial cell

transduction in rat.[18,26] Injection of AAV6-EGFP-TAD (subsequently referred to as AAV6-TAD) or control AAV6-EGFP into L4 and L5 DRGs of naïve rats did not alter thermal or mechanical sensitivity of the ipsilateral plantar skin during the four weeks postinjection observation period (Supplementary S2), nor did vector application appear to affect ambulation or limb posture, as evaluated by general observation.

Sensory neuron expression of EGFP-TAD inhibits TRPV1 channel activity

TRPV1 responds to capsaicin by increased nonselective Ca^{2+}-permeability. We therefore examined the functional efficacy of EGFP-TAD expression in the primary sensory neurons by recording capsaicin-induced changes in intracellular calcium ($[Ca^{2+}]_c$) and whole-cell calcium current (I_{Ca}). Small to medium sensory neurons (25–40 μm in diameter) were cultured from L4/L5 DRGs of naïve animals and from L4/L5 DRGs four weeks after they had been injected with either AAV6-TAD or AAV6-EGFP. Fura-2 imaging showed that transient increases in $[Ca^{2+}]_c$ after stimulation with capsaicin (50 and 100 nM) were similar in naïve neurons and neurons expressing only EGFP (peak $[Ca^{2+}]_c$ of 50 nM capsaicin: naïve neurons 1.02 ± 0.6 μM, neurons expressing EGFP 1.25 ± 0.2 μM, $p > 0.05$; peak $[Ca^{2+}]_c$ of 100 nM capsaicin: naïve neurons 0.92 ± 0.3 μM, neurons expressing EGFP 0.95 ± 0.3 μM, $p > 0.05$) (Figure 1(a)). In contrast, neurons expressing EGFP-TAD showed a significantly decreased capsaicin-stimulated $[Ca^{2+}]_c$ peak (0.46 ± 0.3 μM and 0.26 ± 0.3 μM for 50 and 100 nM of capsaicin, $p < 0.001$ and $p < 0.01$ vs. neurons expressing EGFP). Electrophysiological recording showed large inward capsaicin-induced currents in control neurons, and consistent with the $[Ca^{2+}]_c$ data, peak inward current density was not different between neurons from naïve rats and neurons expressing EGFP (naïve neurons: 8.52 ± 1.4 pA/pF, neurons expressing EGFP: 8.90 ± 1.73 pA/pF,

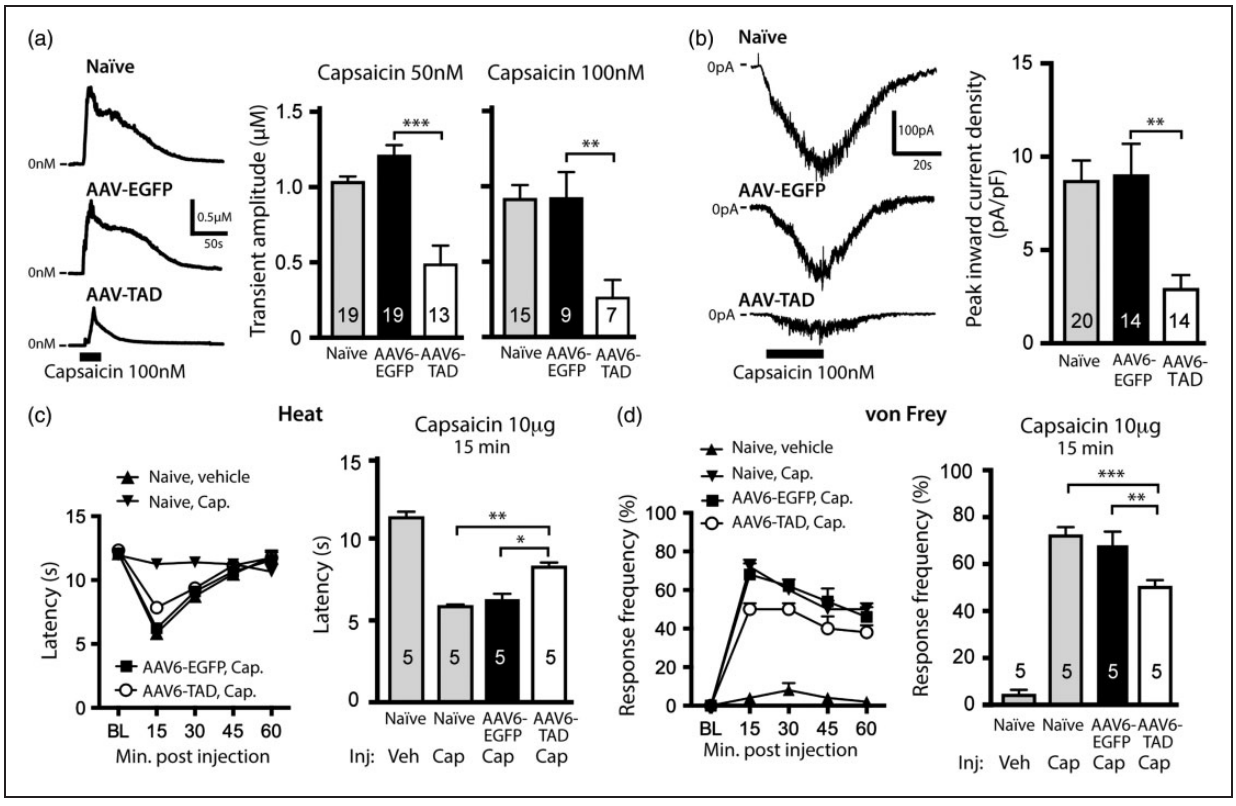

Figure 1. Expression of EGFP-TAD in sensory neurons inhibits TRPV1 channel activity and reduces response to plantar capsaicin. (a) and (b) Representative recording traces of intracellular calcium ($[Ca^{2+}]_c$) (a) and whole-cell calcium currents (I_{Ca}) (b) activated by 100 nM of capsaicin (Cap) in dissociated primary sensory neurons from naïve rat, and from AAV6-EGFP neurons and AAV6-TAD expressing neurons. Summarized data of Ca^{2+} transient exposed to 50 and 100 nM Cap (right panel of (a)) and whole-cell I_{Ca} response to 100 nM Cap (right panel of (b)) are shown as bar charts. Applications of Cap are shown in black bars. (c) and (d) Measurements of heat withdrawal latencies (c) and mechanical withdrawal frequency ((d), single 10 g von Frey filament) after hindpaw subcutaneous 10 μg Cap. Left panels are time course after injection of Cap, and right panels are summarized results at 15 min after injection. *$p < 0.05$, **$p < 0.01$, and ***$p < 0.001$.

$p > 0.05$), whereas TAD expressing neurons showed significantly attenuated capsaicin-induced current (2.89 ± 0.76 pA/pF, $p < 0.01$ compared to EGFP expressing neurons) (Figure 1(b)). These observations demonstrate that the physiological response to TRPV1 channel activation is reduced in sensory neurons expressing EGFP-TAD.

Intradermal administration of capsaicin activates TRPV1 and sensitizes the skin to noxious mechanical and thermal stimuli.[42] To further test the efficacy of AAV6-TAD, we examined heat and mechanical responses after intraplantar capsaicin (10 μg) in naïve animals and those injected with AAV6-EGFP or AAV6-TAD (28 days after injection, except for two rats at 29 days for AAV-GFP and one rat 26 days after AAV-TAD; five animals per group). The time latency to withdraw the paw from radiant heat projected on the plantar skin was markedly reduced after intradermal capsaicin in naïve animals, and this was unchanged in rats with AAV6-EGFP injected in the ipsilateral L4 and L5 DRGs. However, this hypersensitivity to heat was diminished in rats injected with AAV6-TAD (Figure 1(c)). To test the effect of plantar capsaicin on mechanical sensitivity, the rate of withdrawal response to plantar stimulation with a 9 g von Frey filament was measured. Capsaicin increased the response frequency in naïve and AAV6-EGFP injected rats, but this mechanical hypersensitivity was diminished in AAV6-TAD injected rats (Figure 1(d)). Together, these results indicate that AAV-directed selective expression EGFP-TAD in DRG neurons leads to desensitization of TRPV1 neurons to capsaicin and suggest an analgesic potential of TAD against both heat and mechanical hypersensitivity.[43,44]

Neuropathic pain is alleviated by AAV-encoded TAD expression

To test the hypothesis that AAV-mediated TAD expression selectively in the primary sensory neurons can prevent neuropathic pain following peripheral nerve injury, rats were injected with either AAV6-TAD or AAV6-EGFP (2.0×10^{10} viral particles per DRG) at the same time as performing TNI (referred hereafter to this design as Early Treatment). Nearly all of the sciatic DRG perikarya reside in the L4 and L5 DRGs,[29] so these two DRGs were injected. Sensitivity to heat and mechanical cutaneous stimulation was evaluated prior to TNI and DRG injection and was followed for eight weeks after injection of the vectors. Results showed that, after TNI surgery, all animals injected with AAV6-EGFP developed elevated sensitivity to heat, mechanical allodynia to innocuous mechanical stimulation (von Frey), and hyperalgesia to noxious mechanical stimulation (Pin), which lasted the full period of observation (Figure 2(a)). Animals injected with AAV6-TAD also exhibited hypersensitivity to heat stimulation and mechanical allodynia and hyperalgesia after TNI. However, hypersensitivity to these stimuli was significantly attenuated compared to the animals injected with the AAV6-EGFP control vector (Figure 2(a)). These findings suggest that application of AAV6-TAD early in the development of injury-induced neuropathic pain limits the development of hypersensitivity to heat and mechanical stimulation.

We next evaluated the ability of AAV-mediated TAD expression to reverse established neuropathic pain (termed Late Treatment). In this design, rats received intraganglionic vector injection (L4/L5 DRGs) 14 days after TNI, followed by seven weeks of sensory behavior evaluation. Results showed that there was no significant effect on mechanical hyperalgesia (Pin; Figure 2(b)), and that the average degree of hyperalgesia (%) for the final four determinations of hyperalgesia (days 35 through 56 after TNI) was less for the early treatment ($30 \pm 4\%$) than for late treatment ($40\% \pm 7\%$; $p = 0.029$), which indicates that early treatment is important for mechanical hyperalgesia. The attenuating effect of Late Treatment on mechanical allodynia (von Frey) was significant (von Frey, Figure 2(b)), but allodynia during the final four determinations was nonetheless greater after Late Treatment 4.0 ± 0.4 g than when AAV6-TAD was delivered early (7.4 ± 0.7 g; $p = 0.0006$). For heat hypersensitivity, Late Treatment with AAV6-TAD substantially reversed latency (Figure 2(b)), and the average degree of latencies for the final four determinations in Late Treatment were comparable (9.5 ± 0.1 s) to the average latencies in Early Treatment (9.7 ± 0.05 s; $p = 0.0488$), indicating that AAV6-TAD retains analgesic efficacy against hypersensitivity to heat even in established neuropathic pain.

AAV6-TAD produces long-lasting transgene expression

Immunohistochemical characterization on L4/L5 DRGs, lumbar spinal cord, and hindpaw glabrous skin from rats eight weeks after TNI plus Early Treatment showed that AAV6-TAD efficiently and persistently transduced DRG neurons that include sub-populations positive for the TRPV1, the small peptidergic neuron marker calcitonin gene-related peptide, and the nonpeptidergic small neuron marker isolectin B4 (IB4), as well as large-sized neurons immunolabeled by NF-200 (Figure 3(a) to (e)). In neurons of all size groups, TRPV1 expression was found in neurons that were highly co-labeled for EGFP-TAD in sections from the TNI group, suggesting that TRPV1 is expressed not only in the non-myelinated and thinly myelinated C- and Aδ-fibers but also in the myelinated Aβ-fibers following nerve injury.[45] This may in part explain the observed effectiveness of AAV6-TAD treatment on mechanical hypersensitivity in TNI animals. The *in vivo* transduction rate for

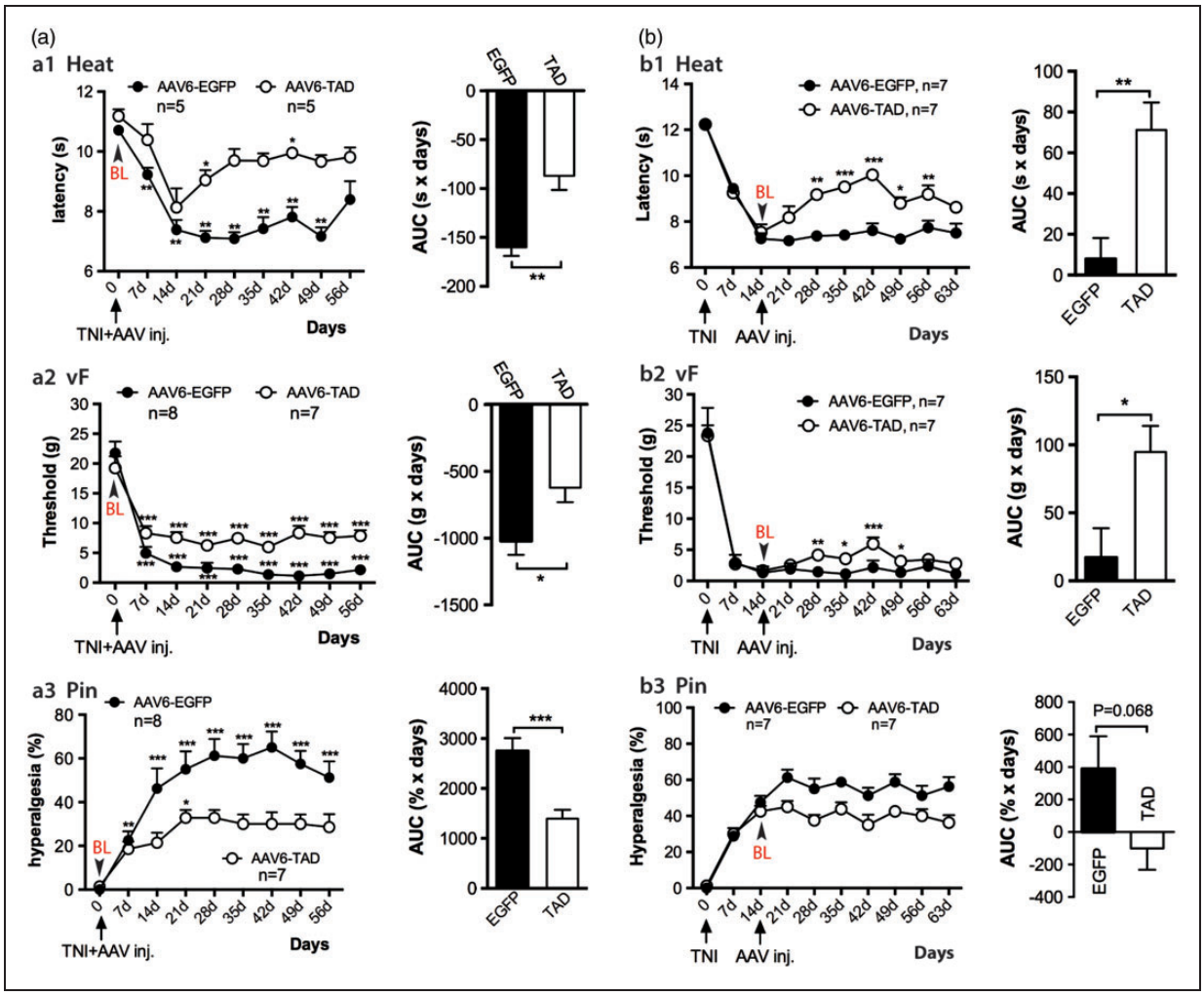

Figure 2. Therapeutic efficacy of intraganglionic AAV6-TAD in TNI-induced neuropathic pain rat. (a) Early Treatment. After the baseline (BL, day 0) behavioral determinations, injection of AAV vectors into the fourth and fifth lumbar (L) DRGs was performed immediately after surgical tibial nerve injury (TNI). Panels of a1 to a3 show the time courses for the group averages of sensitivity to Hargreaves test (Heat, a1), innocuous punctate mechanical stimulation (von Frey, a2), and hyperalgesia behavior after touch with a pin (Pin, a3) before and after DRG injection of either AAV6-EGFP ($n = 8$) or AAV6-TAD ($n = 7$) as indicated. Right panels of a1 to a3 show averaged area under the curve (AUC, calculated from a baseline at day 0) following TNI and vector injection for Heat, von Frey, and Pin. Heat data were obtained from different group animals. *$p < 0.05$, **$p < 0.01$, ***$p < 0.001$ for comparisons to day 0 (a1–a3) and for comparisons between groups (AUCs). (b) Late Treatment. The rats 14 days after TNI received vector intraganglionic injection. The behavior at day 14 following TNI (just before injection) are used as the baseline (BL) for comparison to subsequent days. Panels of b1 to b3 show the time courses for the group averages of Heat (b1), von Frey (b2), and Pin (b3) before and after DRG injection of either AAV6-EGFP ($n = 7$) or AAV6-TAD ($n = 7$) as indicated. Right panels of b1 to b3 show averaged area under the curve (AUC, calculated from the baseline at day 14 after TNI) for seven weeks following vector injection for heat (b1), von Frey (b2), and Pin (b3). *$p < 0.05$, **$p < 0.01$, ***$p < 0.001$ for comparisons to BL (b1–b3) and for comparisons between groups (AUCs).

AAV6-TAD at eight-week after TNI followed by vector injection was $51\% \pm 8\%$ of total neuronal profiles (positive for β3-tubulin) within sections showing the entire ganglion ($n = 3$ DRGs, five sections per DRG). Examination of the corresponding spinal cord revealed that EGFP-TAD fibers terminate predominantly in the superficial laminae, some in deeper laminae, as well as dorsal column, of ipsilateral dorsal horn (DH) (Figure 3(f)), whereas no EGFP-TAD signal was observed in DH neurons. Abundant EGFP-TAD was also detected in the skin sections of ipsilateral hindpaws (Figure 3(g)), but no transgene product was detected in brain and liver (Data not shown). These findings validate stable expression of the transgene product (EGFP-TAD) restricted in the peripheral sensory nervous pathway ipsilateral to injection. Similar patterns of EGFP expression in the DRG neurons and their axonal projections were detected following AAV6-EGFP injection

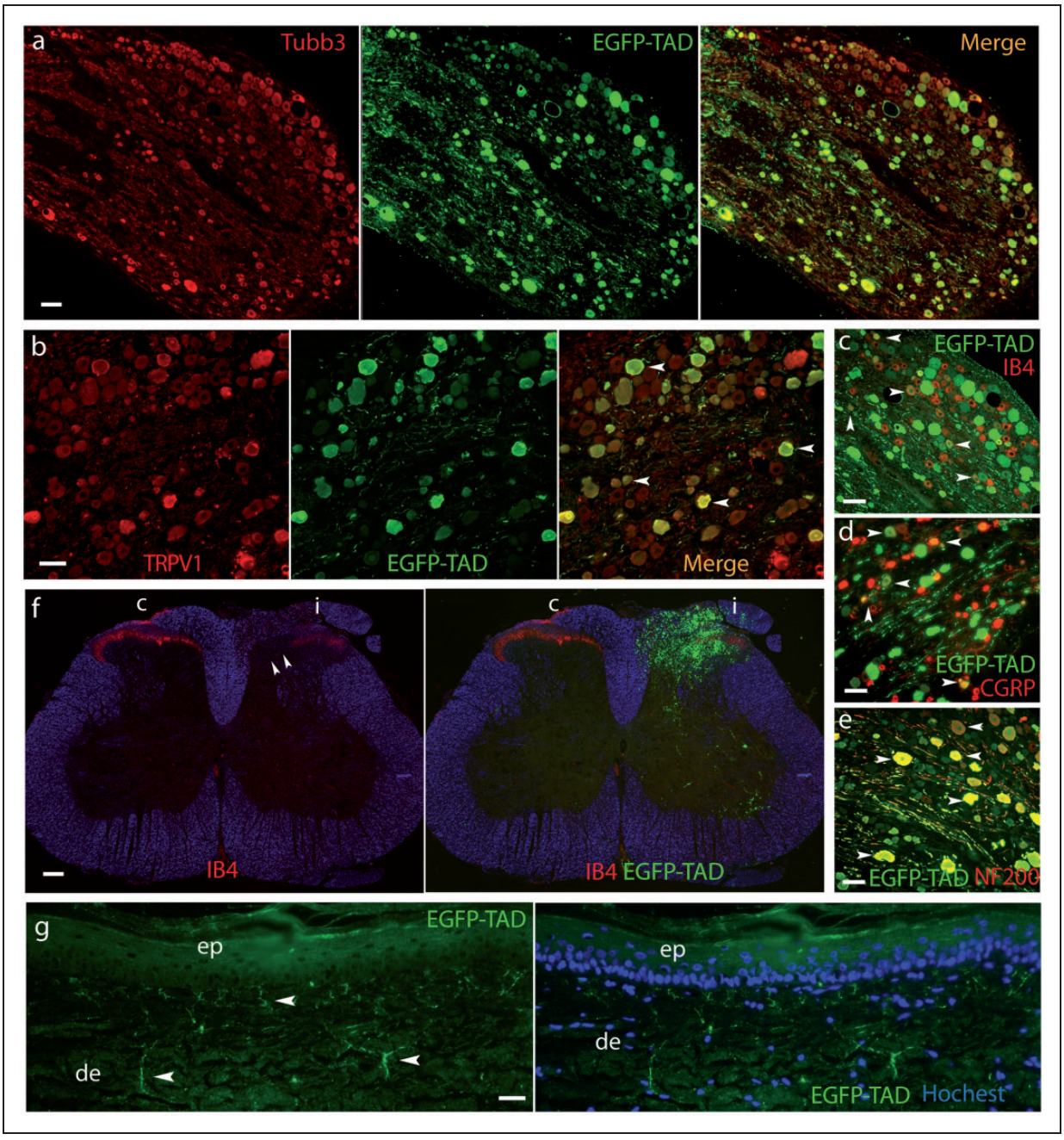

Figure 3. AAV6-directed long-term expression of fluorescent TAD in DRG neurons. DRG sections from Early Treatment TNI rats in which AAV6-TAD was injected eight weeks previously were immunostained with antibodies to GFP (green) and counterstained by pan neuronal marker Tubb3 (a), TRPV1 (b), CGRP (c), IB4 (d), or NF-200 (e). Arrowheads point to examples of co-labeled neurons. Lumbar spinal cord axial sections from rats eight weeks following TNI+AAV6-TAD injection show reduced IB4 staining (red, arrowheads) in the medial dorsal horn, representing the loss of hind limb tibial nerve afferents after TNI ((f), left panel), and EGFP-TAD expression predominantly in ipsilateral DH with few fibers extending to the ventral horn ((f), right panel). White matter of SC was pseudocolored to blue. The EGFP-TAD positive sensory fibers (green; Hoechst counterstain in blue) were also widely observed in the subcutaneous layer, and in the dermis and dermoepidermal junction (arrowheads) in the sections from hindpaw glabrous skin (g). Scale bars: 100 μm for all images.

(Supplementary S3), as previously reported in literature.[26]

Western blots of DRG tissue homogenates prepared from rats eight weeks after TNI plus vector injection (Early Treatment) identified the EGFP-TAD fusion protein based on the size disparity between EGFP-TAD and EGFP, indicating stability of EGFP-TAD protein *in vivo* during eight weeks of expression (Figure 4).

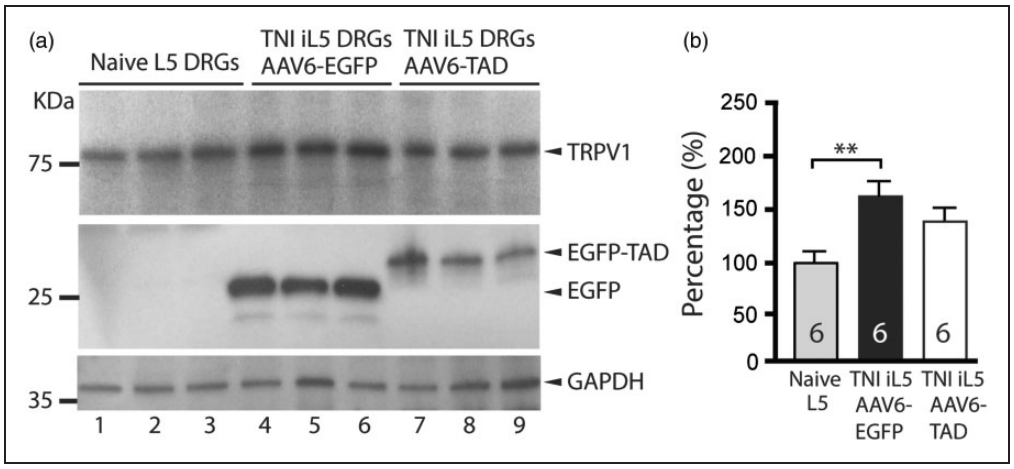

Figure 4. Western blots of TRPV1 and transgene expression. (a) Representative immunoblots of TRPV1 (top panel), EGFP (middle panel), and GAPDH (bottom panel) on the lysates of the L5 DRGs from sham-operated rats (lanes 1, 2, and 3) and the ipsilateral L5 DRGs at eight-week after TNI and Early Treatment, injected by AAV6-EGFP (lanes 4, 5, and 6) or AAV6-TAD (lanes 7, 8, and 9). Arrows point to the expected size bands for TRPV1, EGFP-TAD or EGFP, and GAPDH as a loading control. (b) Bar chart is the results of densitometry analysis ($n = 6$ per group, $^{**}p < 0.01$).

TRPV1 protein level in TNI-DRGs injected with AAV6-TAD was not different from levels in TNI-DRGs injected with AAV6-EGFP or in sham control DRGs (Figure 4, $n = 6$ per group). However, TRPV1 protein level in TNI-DRGs (L5) injected with AAV6-EGFP was significantly elevated compared with control DRGs. To verify this TRPV1 elevation in TNI DRG was not due to vector injection, immunoblotting and immunohistochemistry analyses were performed in the ipsilateral L5 DRGs harvested four weeks after TNI alone. After injury, TRPV1 immunopositivity appeared in all neuronal size groups, in contrast to control DRG section in which TRPV1 expression was mainly limited to small-sized neurons (Figure 5(a) to (c)). The relative TRPV1 protein level was $59\% \pm 23\%$ higher after TNI compared to control DRGs ($n = 6$ per group, $p < 0.01$; Figure 5(d)). It has previously been reported that spinal nerve ligation upregulates TRPV1 heat function in injured IB4-positive DRG neurons,[46] that partial peripheral nerve injury elevates TRPV1 expression in the undamaged ganglia neurons,[47,48] and that both TRPV1 mRNA and protein are upregulated in L5 DRGs ipsilateral to spared nerve injury.[49,50] TNI produces DRGs with co-mingled injured and uninjured axons, so our showing elevated TRPV1 level following TNI are compatible with prior findings and support the importance of TRPV1 in sensitization and pain transmission following TNI nerve injury.[48]

Effect of AAV6-TAD on DH neuronal activity

Pain signaling is supported by TRPV1 not only by initiating activity in peripheral sensory neuron terminals but also by aiding neurotransmission in the spinal cord DH. TRPV1 is enriched in the central presynaptic terminals of the DH, where it facilitates the transmission of noxious stimuli,[51] and nerve injury-induced TRPV1 receptor upregulation occurs at central presynaptic sites of primary afferents leading to an enhancement of excitatory signaling in the spinal cord.[52] Prior studies of animals with neuropathic pain have observed abnormal activity in neurons of the lamina V area of the DH, including elevated spontaneous activity and evoked activity following cutaneous stimulation.[53–55] We therefore examined firing properties of deep DH neurons in TNI rats after Late Treatment with AAV6-TAD. Extracellular recordings of evoked and spontaneous activity of spinal cord DH neurons were obtained from anesthetized TNI rats at a timepoint nine weeks after TNI and seven weeks after injection of either AAV6-EGFP or AAV6-TAD. Total spontaneous activity was recorded ipsilateral to the TNI at two different longitudinal locations within the L4/L5 levels of the spinal cord and within the laminae IV to VI at four prechosen depths from the surface at each longitudinal location. This design was used in order to avoid sampling bias towards active areas. The activity of 51 such sites from TNI rats treated by AAV6-TAD ($n = 8$) and 55 sites from the TNI rats by AAV6-EGFP injection ($n = 7$) were recorded. This showed decreased spontaneous activity in AAV6-TAD-treated TNI animals (3.2 ± 0.1 spikes/s) compared to recordings from AAV6-EGFP-treated TNI animals (3.8 ± 0.2 spikes/s, $p < 0.05$; Figure 6(a)). In the same animals, activity evoked by receptive field mechanical stimuli (brush, graded von Frey filaments, and pinch by two graded vascular clamps) was used to identify single units as wide dynamic range neurons. Comparison of these evoked responses between animals injected with

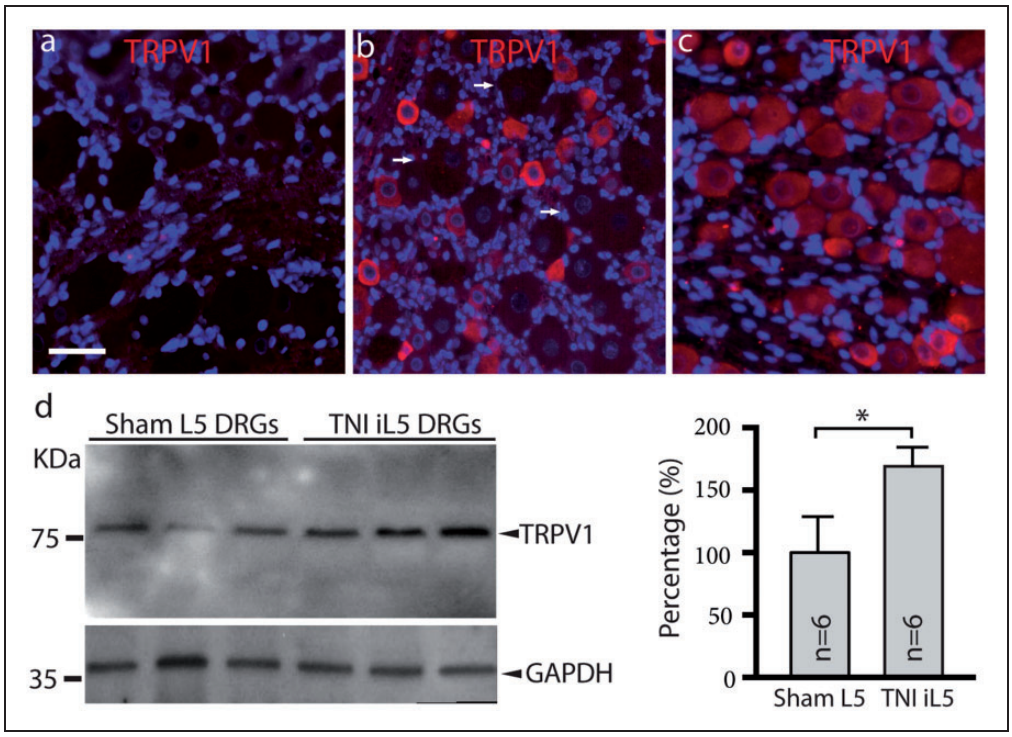

Figure 5. TRPV1 IHC phenotype and protein expression in DRGs following TNI. (a) to (c) Representative IHC images show negative control without first antibody (a), and TRPV1 immunopositivity (red) in small-sized neurons in sham injury control DRG section ((b); arrows indicate that large neurons, outlined by Hoechst 33258 stained satellite glial cells, are TRPV1 negative), while neurons of all sizes are immunolabeled for TRPV1 in the section from DRG ipsilateral to TNI 28 days after injury (c). Sections are counterstained with Hoechst 33258 (blue). (d) Immunoblots of TRPV1 and GAPDH on L5 DRG lysates prepared from the rats with mechanical allodynia and hyperalgesia 28 days after TNI and control samples as indicated. Bar chart in right panel of (c) is the results of densitometry analysis (*$p < 0.05$).

AAV6-TAD versus AAV6-EGFP, however, did not reveal significant differences (Figure 6(b)).

Discussion

Our general aim is to develop primary sensory neuron-specific AAV-encoded iPA treatment for neuropathic pain, for which TRPV1 was chosen as a target because it is a critical signaling node for pain transduction and transmission in primary sensory neurons.[7] Additionally, this genetic approach offers a unique opportunity to test the role of DRG neurons in neuropathic pain. The results presented here validate that AAV6-delivered, sensory neuron-specific expression of a fluorescent TAD, consisting of a 38mer iPA designed to interrupt TRPV1 subunit assembly, can reduce TRPV1 activity in primary sensory neurons. Furthermore, single injection of AAV6-TAD into lumbar DRGs leads to long-term TAD expression and sustained attenuation of neuropathic hypersensitivity to both heat and mechanical stimulation. A detailed mechanistic analysis remains to be documented, but analgesic effects of AAV-encoded TAD in DRG neurons may be mediated by disrupting TRPV1 function at multiple sites along the entire neuron, including decreased ectopic activity in the soma, modulated impulse generation at the peripheral terminals, and inhibited presynaptic neurotransmission in the DH.[56]

Overall, our findings add further evidence that support primary sensory neuron TRPV1 as an important target for pain management. Other genetic-based and ligand-based TRPV1 silencing/ablating strategies have been proposed for targeting sensory neurons, such as TRPV1 RNA interference and combined application of resiniferatoxin and lidocaine derivative QX314 treatment,[49,57,58] which efficiently provide relief of pathological pain. However, RNA interference gene knockdown results in posttranscriptional silencing of all TRPV1 functions, and QX314 can produce cytotoxicity.[57,59] In contrast, the AAV-iPA strategy may provide a more finely tuned regulation of neuronal function because it blocks only the selected protein–protein interaction, while leaving other roles of this multifunctional protein unaffected, such as TRPV1's neuroprotective role.[60]

TRPV1 not only encodes noxious heat in primary sensory neurons[3] but also responds to chemicals that trigger pain after neuroinflammation[5] and additionally

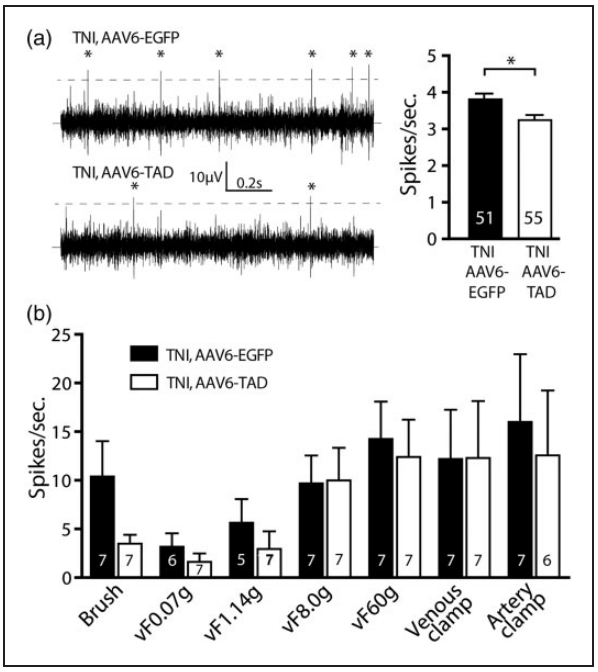

Figure 6. Electrophysiological recordings of dorsal horn neuronal activity. (a) Sample traces of spontaneous activity recorded from ipsilateral DH after vector Late Treatment are shown in the left panel (dotted line indicating threshold, *showing counted action potentials), and group data in right panel. Spontaneous activity for AAV6-TAD-treated TNI animals (55 recording sites in eight rats) was significantly less than the rate recorded from AAV6-EGFP-treated TNI animals (51 recording sites in seven rats; $*p < 0.05$). (b) During natural mechanical stimulation by brush, von Frey fibers of graded force, and pinch of the receptive field by graded clamps, activity evoked in identified wide dynamic range neurons increased with intensity of the stimulus. Comparison of these evoked responses recorded from ipsilateral DH between animals injected with AAV6-TAD versus AAV6-EGFP did not reveal significant differences.

is implicated in neuropathic pain.[61] Our results show that targeting DRG TRPV1 signaling specifically by TAD is effective for attenuating heat hypersensitivity and also can diminish mechanical hypersensitivity. Convergent evidence suggests that TRPV1 may function as a molecular integrator for multiple types of sensory inputs including mechanotransduction,[43,62,63] although this is not yet resolved. Previous reports show that intraganglionic resiniferatoxin induces analgesia for both thermal and mechanical stimulation, while intrathecal AAV-shRNA targeting TRPV1 produces heat analgesia but mechanical pain sensation remained intact.[49] Pain alleviation by targeting sensory neurons with TAD interference may be mechanistically different from these various approaches. Specifically, it has been shown that the C-terminus of TRPV1 contains overlapping segments that are necessary for interaction with multiple molecules that are involved in pain pathology by various mechanisms. Therefore, there should be interacting effects of signal transduction components by our 38mer TAD motif.[64] These may involve, for example, the putative binding sites for calmodulin,[21] A-kinase anchoring proteins,[17] anoctamin,[11] and lipid mediators such as endovanilloids and lysophosphatdic acid,[65] as well as phosphorylation sites.[66] Furthermore, the TAD domain of TRPV1 is highly conserved with the corresponding C-terminal amino acid sequence of other TRPV family members, especially TRPV4 that has 63% residue identities with TRPV1-TAD (Figure 7),[67,68] although other transient receptor potential members lack this sequence homology. Thus, the functional relevance of AAV-mediated TAD interference might extend beyond TRPV1 channel. TRPV4 is known to mediate mechanotransduction[69] and plays a crucial role in a painful peripheral neuropathy.[70,71] TRPV4 is reported highly colocalized with TRPV1 in DRG neurons,[72] and biochemical and biophysical evidence also indicate a close proximity between TRPV4 and TRPV1 in DRG neurons.[73] Therefore, a detailed examination of the ion channels and receptors involved in the pathophysiology of pain conditions related to the TRPV1 interactome is a suitable high priority for future investigation. It was not our goal to identify the subgroup of neurons that account for the therapeutic efficacy of our AAV iPA approach. Future research can employ AAV serotypes with tropism for distinct neuronal populations and selective promoters to isolate the one or more specific neuronal populations that need to be treated. Additionally, as there is 30% to 60% homology for TRPV2, TRPV3, and TRPV4 at the TAD, compared to TRPV1, we cannot attribute the entire analgesic efficacy of EGFP-TAD to action only on TRPV1.

Our preliminary electrophysiological observations show that AAV6-TAD reduces spontaneous activity of DH neurons in the deep laminae of the nucleus proprius. This may reflect an underlying therapeutic mechanism contributing to the analgesic effect of AAV6-TAD since spontaneous activity of these neurons is a feature of various neuropathic pain conditions.[74] Spontaneous activity in DH neurons could be triggered by activity originating in peripheral sensory fibers following injury.[53–55] We did not identify an effect of AAV6-TAD on firing evoked by graded mechanical stimuli, although this negative finding could result from the inherently heterogeneity of sensory units and resulting high variance in the data. Additionally, these recordings were performed at a late timepoint when the effect of AAV6-TAD treatment was decreasing, and in the Late Treatment experimental design. Both of these features diminished the efficacy of AAV-TAD treatment shown in behavioral evaluations, so electrophysiological differences from the AAV-EGFP-treated controls would be expected to be limited in these animals. A greater effect

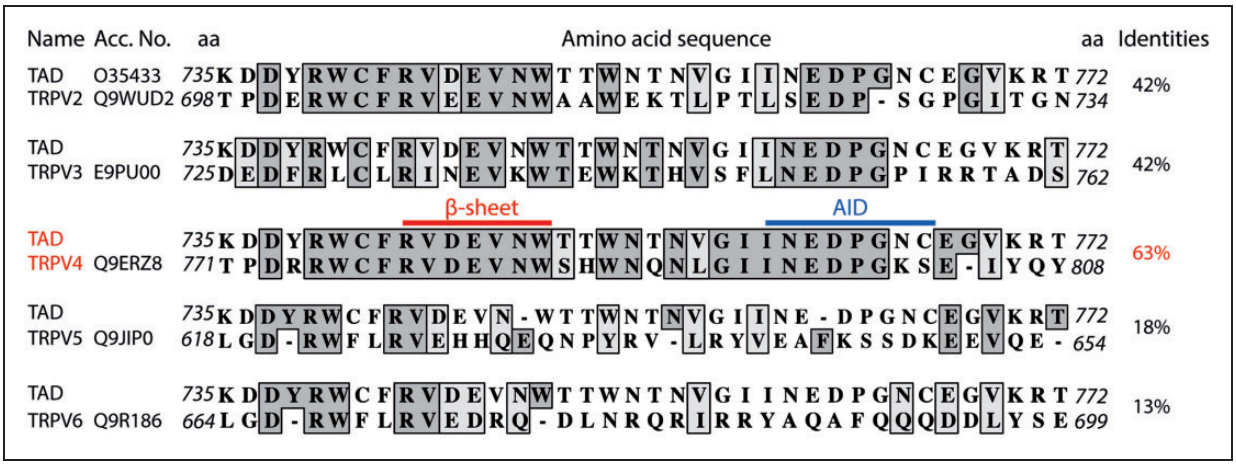

Figure 7. Sequence alignment. Amino acid sequence alignments are plotted for 38mer TRPV1 TAD amino acid sequence with the corresponding sequences from the C termini of TRPV2, TRPV3, TRPV4, TRPV5, and TRPV6 from rat as indicated by UniProtKB Acc. No. (http://www.expasy.org). Initial amino acid of the shown sequence is 698, 725, 771, 618, and 664 for TRPV2, TRPV3, TRPV4, TRPV5, and TRPV6, respectively. Identical residues between TRPV1 TAD and TRPV2-6 are highlighted in dark gray, with the percentage of identity shown on the right, respectively. A cryo-EM mapped β-sheet and a proposed autoinhibitory domain (AID) in TRPV1 and TRPV4 are highlighted.[36,68]

of AAV6-TAD on DH neuron activity might have been seen in Early Treatment animals, and at earlier timepoints. Nonetheless, the observation of diminished spontaneous activity despite these limitations may indicate limiting such activity may be a critical feature of AAV6-TAD analgesia.

We observed analgesic efficacy in two experimental designs that reflect possible clinical application. Administering AAV6-TAD at the time of the injury could be employed clinically when nerve injury is an unavoidable result of surgery, such as limb amputation. Administering AAV6-TAD after a neuropathic pain state is established represents the more typical clinical setting. Although we saw an incomplete analgesic effect of AAV6-TAD, improved efficacy could be achieved by increasing transduction efficiency with repeated injections. Generally, a gene therapy approach based on anatomically targeted AAV delivery of iPAs for controlling specific protein–protein interactions in sensory neurons has high potential for translation into a clinically useful modality in treating chronic pain. AAV has a very favorable safety profile,[75,76] and there is a growing experience of clinical application using this vector. The high specificity of iPAs should limit off-target effects. Intraganglionic injections are a minimally invasive procedure that is routinely performed by appropriately trained physicians. The fact that the widely used procedure of foraminal injection (also known as selective spinal nerve block) commonly results in intraganglionic injection[28] but nerve damage is rare attests[77,78] to the safety of injecting within the DRG. Ultimately, the broad range of known protein–protein interactions involved in pain signaling[10,13] may allow substantial control of sensory neuron pain signaling by AAV-delivered iPAs.

Author's Contributions

HY and QHH conceived and designed the experiments. HY, HX, ZL, FW, GF, CJR, DC, and QHH conducted the experimental investigation and developed methodology. HY, HX, GF, BP, and QHH analyzed the data. Funding acquisition by QHH and HY. HY, QHH, and CJS wrote the paper. HX and ZL contributed equally to this work.

Declaration of Conflicting Interests

The author(s) declared no potential conflicts of interest with respect to the research, authorship, and/or publication of this article.

Funding

The author(s) disclosed receipt of the following financial support for the research, authorship, and/or publication of this article: This work was supported in part by the grants from the Department of Veterans Affairs Rehabilitation Research and Development (I01RX001940, QH), the Advancing a Healthier Wisconsin (FP00005706, QH and HY), and the National Institute of Neurological Disorders and Stroke (R01NS079626-01, QH). ZL was a recipient of Chinese Scholarship Council. HX and FW were supported in part by the National Key Clinical Specialty Construction Project of China and by Scholarship from Shaanxi University of Chinese Medicine, respectively. CJR was partially supported by NIH T32 GM089586.

References

1. Kennedy J, Roll JM, Schraudner T, et al. Prevalence of persistent pain in the U.S. adult population: new data

from the 2010 national health interview survey. *J Pain* 2014; 15: 979–984.
2. Basbaum AI, Bautista DM, Scherrer G, et al. Cellular and molecular mechanisms of pain. *Cell* 2009; 139: 267–284.
3. Caterina MJ, et al. The capsaicin receptor: a heat-activated ion channel in the pain pathway. *Nature* 1997; 389: 816–824.
4. Vriens J, Nilius B and Voets T. Peripheral thermosensation in mammals. *Nat Rev Neurosci* 2014; 15: 573–589.
5. Caterina MJ, et al. Impaired nociception and pain sensation in mice lacking the capsaicin receptor. *Science* 2000; 288: 306–313.
6. Julius D. TRP channels and pain. *Annu Rev Cell Dev Biol* 2013; 29: 355–384.
7. Patapoutian A, Tate S and Woolf CJ. Transient receptor potential channels: targeting pain at the source. *Nat Rev Drug Discov* 2009; 8: 55–68.
8. Gavva NR, et al. Pharmacological blockade of the vanilloid receptor TRPV1 elicits marked hyperthermia in humans. *Pain* 2008; 136: 202–210.
9. Wong GY and Gavva NR. Therapeutic potential of vanilloid receptor TRPV1 agonists and antagonists as analgesics: recent advances and setbacks. *Brain Res Rev* 2009; 60: 267–277.
10. Jamieson DG, et al. The pain interactome: connecting pain-specific protein interactions. *Pain* 2014; 155: 2243–2252.
11. Takayama Y, Uta D, Furue H, et al. Pain-enhancing mechanism through interaction between TRPV1 and anoctamin 1 in sensory neurons. *Proc Natl Acad Sci U S A* 2015; 112: 5213–5218.
12. Elokely K, et al. Understanding TRPV1 activation by ligands: insights from the binding modes of capsaicin and resiniferatoxin. *Proc Natl Acad Sci U S A* 2016; 113: E137–E145.
13. Rouwette T, et al. Modulation of nociceptive ion channels and receptors via protein-protein interactions: implications for pain relief. *Channels (Austin)* 2015; 9: 175–185.
14. Btesh J, Fischer MJ, Stott K, et al. Mapping the binding site of TRPV1 on AKAP79: implications for inflammatory hyperalgesia. *J Neurosci* 2013; 33: 9184–9193.
15. Fischer MJ, Btesh J and McNaughton PA. Disrupting sensitization of transient receptor potential vanilloid subtype 1 inhibits inflammatory hyperalgesia. *J Neurosci* 2013; 33: 7407–7414.
16. Flynn R, et al. Targeting the transient receptor potential vanilloid type 1 (TRPV1) assembly domain attenuates inflammation-induced hypersensitivity. *J Biol Chem* 2014; 289: 16675–16687.
17. Zhang X, Li L and McNaughton PA. Proinflammatory mediators modulate the heat-activated ion channel TRPV1 via the scaffolding protein AKAP79/150. *Neuron* 2008; 59: 450–461.
18. Fischer G, Pan B, Vilceanu D, et al. Sustained relief of neuropathic pain by AAV-targeted expression of CBD3 peptide in rat dorsal root ganglion. *Gene Ther* 2014; 21: 44–51.
19. Zhang F, Liu S, Yang F, et al. Identification of a tetrameric assembly domain in the C terminus of heat-activated TRPV1 channels. *J Biol Chem* 2011; 286: 15308–15316.
20. Garcia-Sanz N, et al. Identification of a tetramerization domain in the C terminus of the vanilloid receptor. *J Neurosci* 2004; 24: 5307–5314.
21. Numazaki M, et al. Structural determinant of TRPV1 desensitization interacts with calmodulin. *Proc Natl Acad Sci U S A* 2003; 100: 8002–8006.
22. Moiseenkova-Bell VY, Stanciu LA, Serysheva II, et al. Structure of TRPV1 channel revealed by electron cryomicroscopy. *Proc Natl Acad Sci U S A* 2008; 105: 7451–7455.
23. Hellwig N, Albrecht N, Harteneck C, et al. Homo- and heteromeric assembly of TRPV channel subunits. *J Cell Sci* 2005; 118: 917–928.
24. Joseph J, Wang S, Lee J, et al. Carboxyl-terminal domain of transient receptor potential vanilloid 1 contains distinct segments differentially involved in capsaicin- and heat-induced desensitization. *J Biol Chem* 2013; 288: 35690–35702.
25. Huynh KW, et al. Structural insight into the assembly of TRPV channels. *Structure* 2014; 22: 260–268.
26. Yu H, et al. Intraganglionic AAV6 results in efficient and long-term gene transfer to peripheral sensory nervous system in adult rats. *PLoS One* 2013; 8: e61266.
27. Fischer G, et al. Direct injection into the dorsal root ganglion: technical, behavioral, and histological observations. *J Neurosci Methods* 2011; 199: 43–55.
28. Pfirrmann CW, et al. Selective nerve root blocks for the treatment of sciatica: evaluation of injection site and effectiveness–a study with patients and cadavers. *Radiology* 2001; 221: 704–711.
29. Swett JE, Torigoe Y, Elie VR, et al. Sensory neurons of the rat sciatic nerve. *Exp Neurol* 1991; 114: 82–103.
30. Hofmann HA, De Vry J, Siegling A, et al. Pharmacological sensitivity and gene expression analysis of the tibial nerve injury model of neuropathic pain. *Eur J Pharmacol* 2003; 470: 17–25.
31. Lee BH, Won R, Baik EJ, et al. An animal model of neuropathic pain employing injury to the sciatic nerve branches. *Neuroreport* 2000; 11: 657–661.
32. Wu HE, Gemes G, Zoga V, et al. Learned avoidance from noxious mechanical simulation but not threshold semmes weinstein filament stimulation after nerve injury in rats. *J Pain* 2010; 11: 280–286.
33. Lin Q, Li D, Xu X, et al. Roles of TRPV1 and neuropeptidergic receptors in dorsal root reflex-mediated neurogenic inflammation induced by intradermal injection of capsaicin. *Mol Pain* 2007; 3: 30.
34. Yu H, et al. Lentiviral gene transfer into the dorsal root ganglion of adult rats. *Mol Pain* 2011; 7: 63.
35. Grynkiewicz G, Poenie M and Tsien RY. A new generation of Ca2+ indicators with greatly improved fluorescence properties. *J Biol Chem* 1985; 260: 3440–3450.
36. Liao M, Cao E, Julius D, et al. Structure of the TRPV1 ion channel determined by electron cryo-microscopy. *Nature* 2013; 504: 107–112.
37. Brauchi S, Orta G, Salazar M, et al. A hot-sensing cold receptor: c-terminal domain determines thermosensation in transient receptor potential channels. *J Neurosci* 2006; 26: 4835–4840.

38. Gregorio-Teruel L, et al. The integrity of the TRP domain is pivotal for correct TRPV1 channel gating. *Biophys J* 2015; 109: 529–541.
39. Kim YH, et al. TRPV1 in GABAergic interneurons mediates neuropathic mechanical allodynia and disinhibition of the nociceptive circuitry in the spinal cord. *Neuron* 2012; 74: 640–647.
40. Cavanaugh DJ, et al. Trpv1 reporter mice reveal highly restricted brain distribution and functional expression in arteriolar smooth muscle cells. *J Neurosci* 2011; 31: 5067–5077.
41. Han L, et al. A subpopulation of nociceptors specifically linked to itch. *Nat Neurosci* 2013; 16: 174–182.
42. Simone DA, Ngeow JY, Putterman GJ, et al. Hyperalgesia to heat after intradermal injection of capsaicin. *Brain Res* 1987; 418: 201–203.
43. Walder RY, et al. TRPV1 is important for mechanical and heat sensitivity in uninjured animals and development of heat hypersensitivity after muscle inflammation. *Pain* 2012; 153: 1664–1672.
44. Brenneis C, et al. Phenotyping the function of TRPV1-expressing sensory neurons by targeted axonal silencing. *J Neurosci* 2013; 33: 315–326.
45. Zakir HM, et al. Expression of TRPV1 channels after nerve injury provides an essential delivery tool for neuropathic pain attenuation. *PLoS One* 2012; 7: e44023.
46. Vilceanu D, Honore P, Hogan QH, et al. Spinal nerve ligation in mouse upregulates TRPV1 heat function in injured IB4-positive nociceptors. *J Pain* 2010; 11: 588–599.
47. Urano H, Ara T, Fujinami Y, et al. Aberrant TRPV1 expression in heat hyperalgesia associated with trigeminal neuropathic pain. *Int J Med Sci* 2012; 9: 690–697.
48. Hudson LJ, et al. VR1 protein expression increases in undamaged DRG neurons after partial nerve injury. *Eur J Neurosci* 2001; 13: 2105–2114.
49. Hirai T, et al. Intrathecal AAV serotype 9-mediated delivery of shRNA against TRPV1 attenuates thermal hyperalgesia in a mouse model of peripheral nerve injury. *Mol Ther* 2014; 22: 409–419.
50. Koh WU, et al. The preventive effect of resiniferatoxin on the development of cold hypersensitivity induced by spinal nerve ligation: involvement of TRPM8. *BMC Neurosci* 2016; 17: 38.
51. Latremoliere A and Woolf CJ. Central sensitization: a generator of pain hypersensitivity by central neural plasticity. *J Pain* 2009; 10: 895–926.
52. Palazzo E, et al. Moving towards supraspinal TRPV1 receptors for chronic pain relief. *Mol Pain* 2010; 6: 66.
53. Bedi SS, et al. Chronic spontaneous activity generated in the somata of primary nociceptors is associated with pain-related behavior after spinal cord injury. *J Neurosci* 2010; 30: 14870–14882.
54. Kajander KC, Wakisaka S and Bennett GJ. Spontaneous discharge originates in the dorsal root ganglion at the onset of a painful peripheral neuropathy in the rat. *Neurosci Lett* 1992; 138: 225–228.
55. Xie YK and Xiao WH. Electrophysiological evidence for hyperalgesia in the peripheral neuropathy. *Sci China B* 1990; 33: 663–672.
56. Kim YS, et al. Central terminal sensitization of TRPV1 by descending serotonergic facilitation modulates chronic pain. *Neuron* 2014; 81: 873–887.
57. Karai L, et al. Deletion of vanilloid receptor 1-expressing primary afferent neurons for pain control. *J Clin Invest* 2004; 113: 1344–1352.
58. Stueber T, et al. Quaternary lidocaine derivative QX-314 activates and permeates human TRPV1 and TRPA1 to produce inhibition of sodium channels and cytotoxicity. *Anesthesiology* 2016; 124: 1153–1165.
59. Peters CM, Ririe D, Houle TT, et al. Nociceptor-selective peripheral nerve block induces delayed mechanical hypersensitivity and neurotoxicity in rats. *Anesthesiology* 2014; 120: 976–986.
60. Veldhuis WB, et al. Neuroprotection by the endogenous cannabinoid anandamide and arvanil against in vivo excitotoxicity in the rat: role of vanilloid receptors and lipoxygenases. *J Neurosci* 2003; 23: 4127–4133.
61. Malek N, Pajak A, Kolosowska N, et al. The importance of TRPV1-sensitisation factors for the development of neuropathic pain. *Mol Cell Neurosci* 2015; 65: 1–10.
62. Liedtke WB and Heller S. *TRP ion channel function in sensory transduction and cellular signaling cascades frontiers in neuroscience*. Boca Raton, FL: CRC Press, 2007.
63. Yin J and Kuebler WM. Mechanotransduction by TRP channels: general concepts and specific role in the vasculature. *Cell Biochem Biophys* 2010; 56: 1–18.
64. Donate-Macian P and Peralvarez-Marin A. Dissecting domain-specific evolutionary pressure profiles of transient receptor potential vanilloid subfamily members 1 to 4. *PLoS One* 2014; 9: e110715.
65. Nieto-Posadas A, et al. Lysophosphatidic acid directly activates TRPV1 through a C-terminal binding site. *Nat Chem Biol* 2012; 8: 78–85.
66. Jendryke T, et al. TRPV1 function is modulated by Cdk5-mediated phosphorylation: insights into the molecular mechanism of nociception. *Sci Rep* 2016; 6: 22007.
67. Garcia-Sanz N, et al. A role of the transient receptor potential domain of vanilloid receptor I in channel gating. *J Neurosci* 2007; 27: 11641–11650.
68. Loukin SH, Teng J and Kung C. A channelopathy mechanism revealed by direct calmodulin activation of TrpV4. *Proc Natl Acad Sci U S A* 2015; 112: 9400–9405.
69. O'Conor CJ, Leddy HA, Benefield HC, et al. TRPV4-mediated mechanotransduction regulates the metabolic response of chondrocytes to dynamic loading. *Proc Natl Acad Sci U S A* 2014; 111: 1316–1321.
70. Alessandri-Haber N, Dina OA, Joseph EK, et al. Interaction of transient receptor potential vanilloid 4, integrin, and SRC tyrosine kinase in mechanical hyperalgesia. *J Neurosci* 2008; 28: 1046–1057.
71. Alessandri-Haber N, et al. Transient receptor potential vanilloid 4 is essential in chemotherapy-induced neuropathic pain in the rat. *J Neurosci* 2004; 24: 4444–4452.
72. Cao DS, Yu SQ and Premkumar LS. Modulation of transient receptor potential Vanilloid 4-mediated membrane

currents and synaptic transmission by protein kinase C. *Mol Pain* 2009; 5: 5.
73. Kim S, et al. Facilitation of TRPV4 by TRPV1 is required for itch transmission in some sensory neuron populations. *Sci Signal* 2016; 9: ra71.
74. Campbell JN and Meyer RA. Mechanisms of neuropathic pain. *Neuron* 2006; 52: 77–92.
75. Asokan A, Schaffer DV and Samulski RJ. The AAV vector toolkit: poised at the clinical crossroads. *Mol Ther* 2012; 20: 699–708.
76. Pleticha J, et al. Preclinical toxicity evaluation of AAV for pain: evidence from human AAV studies and from the pharmacology of analgesic drugs. *Mol Pain* 2014; 10: 54.
77. Botwin KP, et al. Complications of fluoroscopically guided transforaminal lumbar epidural injections. *Arch Phys Med Rehabil* 2000; 81: 1045–1050.
78. Manchikanti L, et al. A prospective evaluation of complications of 10,000 fluoroscopically directed epidural injections. *Pain Physician* 2012; 15: 131–140.

Supplementary Materials

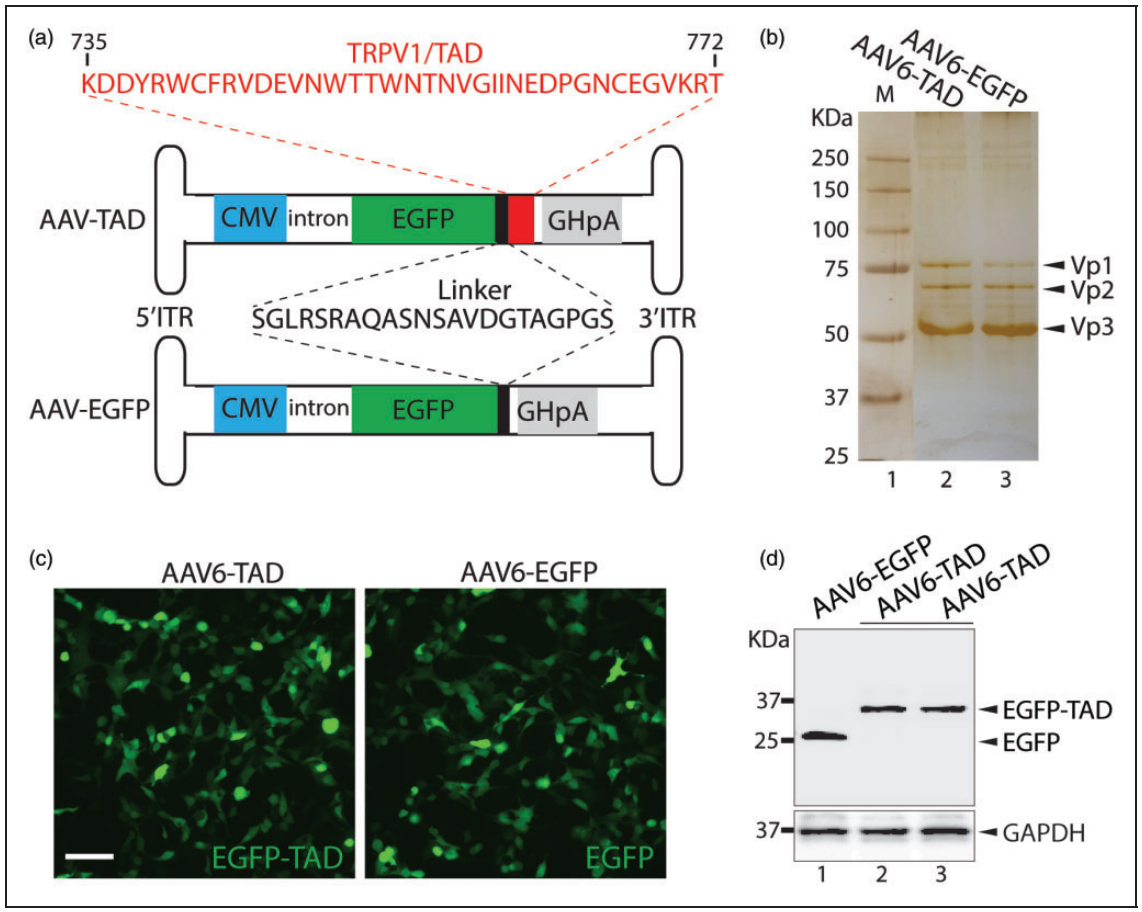

Figure S1. Design and preparation of AAV vectors. (a) Schematic outline of AAV vectors. The vector genomes of AAV-TAD and AAV-EGFP are flanked by AAV2 inverted terminal repeats (ITR). Transgene cassettes encode EGFP-TAD separated by a 22aa linker between EGFP and TAD or EGFP-linker alone downstream of a chimeric intron enhancing transcription driven by the cytomegalovirus (CMV) promoter, and contain polyadenylation signal element from the human growth hormone (GHpA). The amino acid sequence of a 38mer TAD (red) is shown on the top and the linker sequence (back) in the middle of two vectors. (b) Silver stain result of purified AAV6-TAD and AAV6-EGFP. This revealed 3 virion protein bands of Vp1, Vp2, and Vp3, with molecular weight of 87, 72 and 62 KDa, respectively. (c) GFP expression by infectivity estimation upon transduction to HEK293T cells of either AAV6-EGFP or AAV6-TAD at a multiplicity of infection of 10,000. (d) Western analysis on lysates of HEK293T cells transduced by vectors show EGFP immunoreactivity at distinct molecular weights (MWs) for expressed EGFP (lane 1) versus EGFP-TAD (lane 2 and 3). Arrows point to the expected size bands for EGFP-TAD and EGFP (top panel), and glyceraldehyde-3-phosphate dehydrogenase (GAPDH, bottom panel) as a loading control.

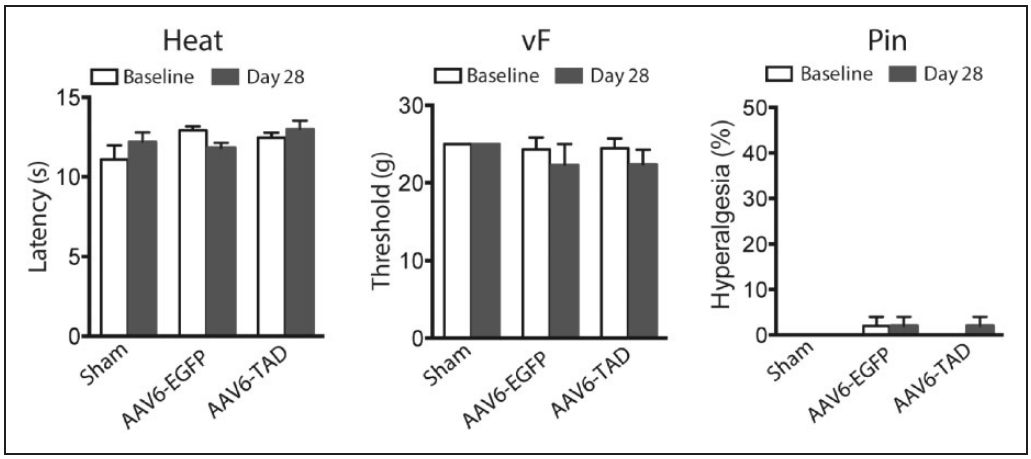

Figure S2. Baseline sensory evaluation after vector injection into DRGs. (a–c) Sensory sensitivity evaluated by Heat, von Frey, and Pin tests after vector injection in non-injured rats. (a) Hargreaves test for heat sensitivity, (b) vF test for innocuous mechanical sensitivity, and (c) Pin test for the evaluation of noxious mechanical sensitivity before and 28-d after vector injection, compared to sham-operated (no injection) animals (n = 5 rats per group).

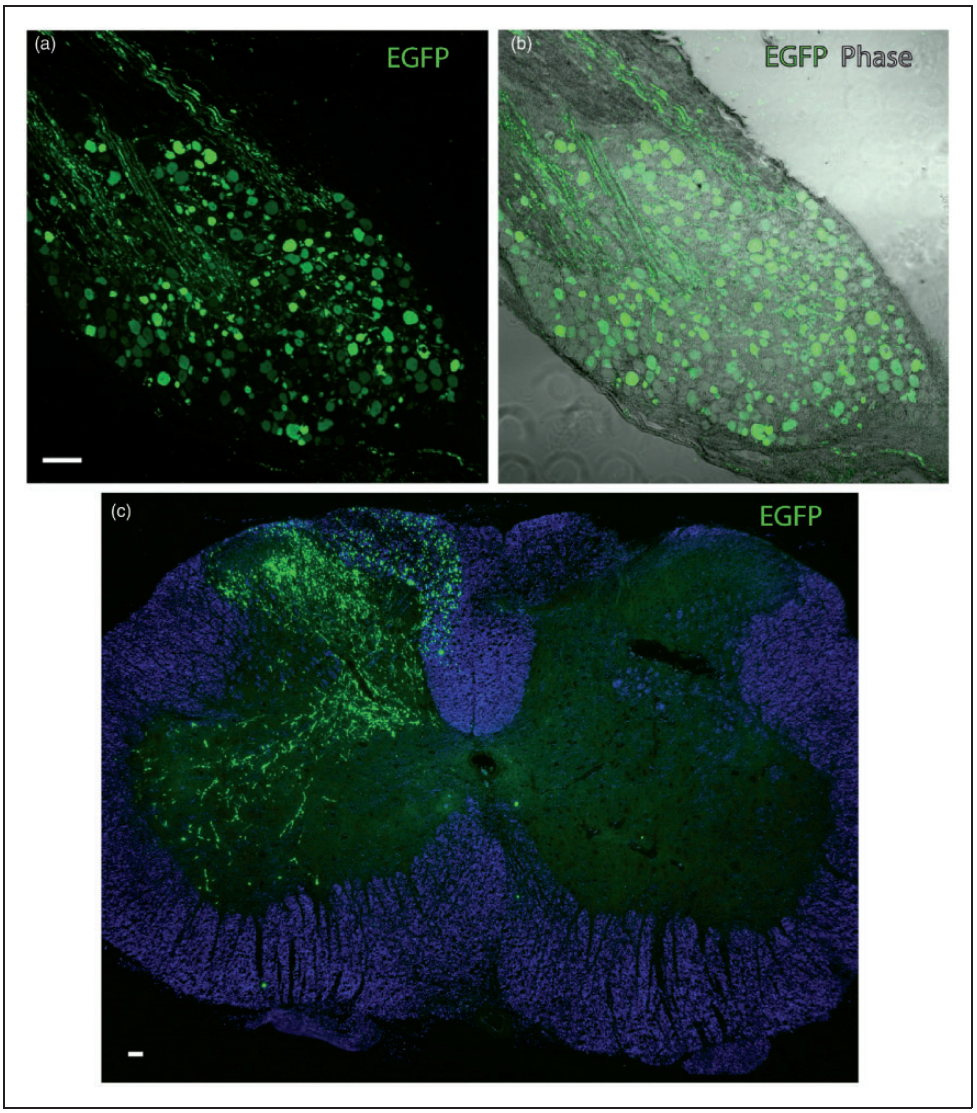

Figure S3. EGFP expression following intraganglionic injection with control vector AAV6-EGFP. Representative IHC images show EGFP expression (a, green) in DRG neurons (b, merged with phase-contrast image) and lumbar spinal cord (c, white matter of spinal cord was pseudocolored to blue) after 8 weeks of intraganglionic injection with AAV6-EGFP. Scale bars: 200 μm.